

## **Performance Assessment of a Floating Power System for the Galway Bay Wave Energy Test Site**

Bret Bosma<sup>1</sup>, Wanan Sheng<sup>2</sup>, Florent Thiebaut<sup>2</sup>

<sup>1</sup>US DOE EERE Postdoctoral Fellow  
Cork, Ireland

E-mail: [bosma@eecs.oregonstate.edu](mailto:bosma@eecs.oregonstate.edu)

<sup>2</sup>Beaufort Research/HMRC  
Cork, Ireland

### **Abstract**

The Galway Bay wave energy test site promises to be a vital resource for wave energy researchers and developers. As part of the development of this site, a floating power system is being developed to provide power and data acquisition capabilities, including its function as a local grid connection, allowing for the connection of up to three wave energy converter devices. This work shows results from scaled physical model testing and numerical modelling of the floating power system and an oscillating water column connected with an umbilical. Results from this study will be used to influence further scaled testing as well as the full scale design and build of the floating power system in Galway Bay.

### **1. Introduction**

The Galway Bay wave energy test site in Ireland promises to be an important resource for wave energy researchers and developers. The site provides the benefit of real sea testing facilities in a relatively benign environment

with a wave climate that is approximately one quarter scale of North Atlantic conditions. Specifically, the site will be a key midpoint for transitioning Wave Energy Converter (WEC) devices from wave tank testing, to operation in the open ocean, and is currently under development.

As part of the development, a Floating Power System (FPS) is being designed to provide power and data acquisition capabilities, including its function as a stable local grid connection point, allowing for the connection of up to three WEC devices. A similar system is discussed in (Lettenmaier, Amon, and von Jouanne 2013).

The FPS will allow developers to focus on their technology, avoiding the need to conduct entire electrical integration at this stage of the development process. The FPS will provide a stable local grid connection for the developers to plug their device into. A potential visualization of the systems components are shown in Fig. 1. A cable to shore connection

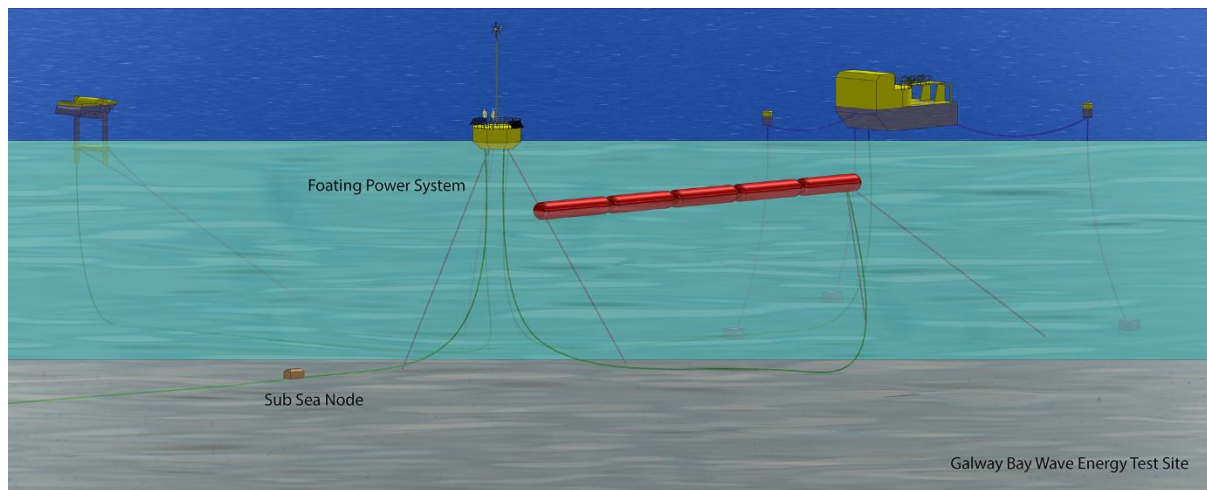


**Figure 1: Rendering of Galway Bay Wave Energy Test Site near Spiddal, Ireland**

will be present, via a subsea node, providing communications and a limited power connection for sensors and data acquisition.

Although the system components are known, there are still many unknowns, especially regarding the mooring and electrical umbilical systems which need to be investigated before implementation. This is being done numerically and through physical scale models to influence the final design of the FPS. Testing of major components at 1:25 scale has been performed and testing at 1:10 scale is planned.

Numerical models of the test site and scaled physical test data, with generic devices, will provide a service toward responsible and effective development of the testing site as well as important information for users of the site.

Several key factors related to the design of the FPS were investigated in this study. The motion response of the FPS itself was analysed along with its interactions with a generic Oscillating Water Column (OWC) WEC. Namely the heave, pitch, and surge motions were analysed and results shown. Watch

circles and device spacing for the components of the test facility were analysed. Mooring analysis was undertaken, investigating typical loads, and estimating maximum loads seen by the two devices. Building on previous work (Bosma 2013), numerical modelling was undertaken using the software package ANSYS AQWA, with a comparison of results with the physical testing for one of the configurations.

Results from this study will influence scaled physical modelling of the devices including wave basin testing to be performed at Plymouth University through funding from the Marinet FP7 project (Lewis 2011). This, in turn, will influence the final design of the wave energy test site in Galway Bay.

## 2. System Overview

A systematic approach was chosen for developing the FPS (Holmes 2012). Design and modelling was first done numerically using ANSYS AQWA. Shapes, dimensions, and mass distributions were iterated until the proposed model was selected. Factors

influencing the hull design include utility, stability, and cost of manufacturing.

### 2.1. Bodies, Mooring, and Umbilical

Two floating structures were built and tested for this project, namely the FPS, and a generic OWC. The bodies were built to 1:25 scale assuming this configuration would be tested in the Galway Bay test site. Each body had an independent mooring system and an umbilical was connected between the bodies for certain tests.

### 2.2. Scaled Floating Power System

The 1:25 FPS scale model has a 200 mm diameter, overall height of 90 mm and a 30 mm draft. Construction of the model was done with a thermoplastic polycarbonate material, sealed, and painted. It had a mass of 766.4 g without the mooring lines attached. The centre of mass is located approximately 29 mm above the water line. Fig. 2 shows the scaled FPS in the wave basin. The markers shown are for the optical tracking system as outlined in a section 4.2.

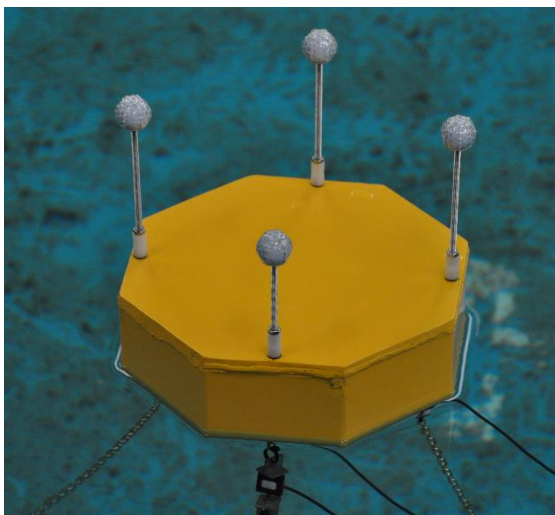


Figure 2: FPS at 1:25 scale in Beaufort Research

### 2.3. Scaled Oscillating Water Column

To test the FPS structure in a realistic scaled environment, a representative prototype WEC was designed and deployed alongside the FPS. A generic OWC type device was chosen and although it was not optimized, it represented a device that could be tested at the final facility. The scaled model has a 300 mm external width, total height of 600 mm and a 400 mm draft.

The main body is constructed from thermoplastic polycarbonate and the float section from high density polyurethane foam which was sealed with a pattern-coat primer. The centre of mass is 122 mm below the water line. The body has a mass of 4836 g without the mooring lines attached. Fig. 3 shows the scaled OWC in the wave basin. The centre rod was used to measure the internal water surface elevation within the OWC chamber. A pressure

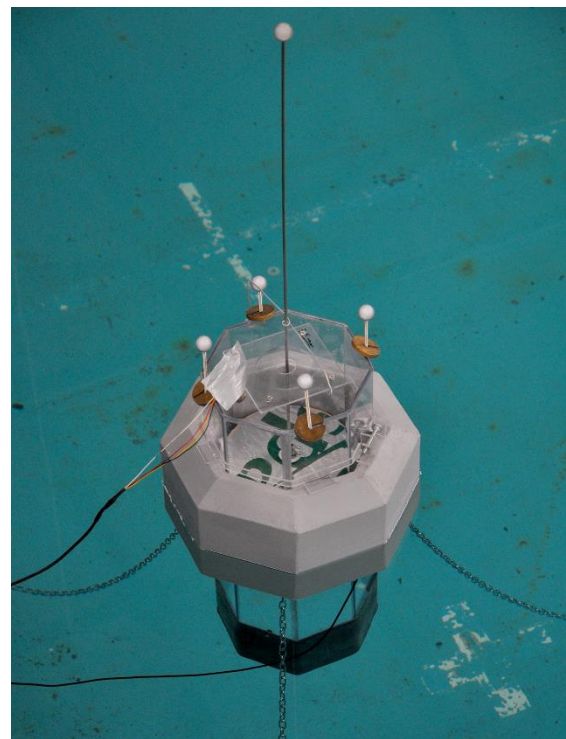


Figure 3: OWC at 1:25 scale in Beaufort Research

sensor was used to measure the pressure inside of the chamber. The orifice in the top of the chamber had a diameter of 25mm.

## 2.4. Mooring Lines

For these tests, mooring for both the FPS and the OWC are a traditional three point catenary mooring system. For both setups, the mooring line length was 3 m and angle between the lines were 120°. The FPS mooring chain has a linear density value of 45.5 g/m and the OWC chain a value of 93.0 g/m. The anchor points were placed 2.6 m from the body centre in plan. Orientation of the mooring lines were changed for the various experiments undertaken. Future tests are planned to compare a compliant taut mooring system to the catenary system.

## 3. Numerical Modelling

Numerical modelling was conducted to simulate the Galway Bay site as close as possible. Through model validation, the goal is to gain confidence in the numerical model to the point where design iterations can be comfortably made. The following is a short overview of the methods used in the numerical models.

The method of potential flow theory has been developed to reliably assess the hydrodynamic performance of ships and ocean platforms over the last century. The method's accurate performance in determining a structure's response to waves has led to its recent application in the development of WECs.

Potential flow theory assumes flow around the structure(s) is irrotational, incompressible, and inviscid. In addition, to simplify the analysis, the wave and the structure motions are assumed to be small in amplitude, so that a fully linear dynamic system can be established, and the

analysis can be done in the frequency domain (details can be found in textbooks (Falnes 2005)(Newman 1977)(Faltinsen 1993)).

In the frequency domain analysis of a potential flow, a velocity potential ( $\varphi$ ) is solved, as it must satisfy the Laplace equation, as

$$\nabla^2 \varphi = 0 \quad (1)$$

where  $\varphi$  is a function of frequency, and the complex amplitude of its velocity components are given by

$$v_x = \frac{\partial \varphi}{\partial x}, v_y = \frac{\partial \varphi}{\partial y}, v_z = \frac{\partial \varphi}{\partial z} \quad (2)$$

For solving the velocity potential in a linear dynamic system, the velocity potential is usually decomposed as follows:

$$\varphi = \varphi_0 + \varphi_D + i\omega \sum_{j=1}^{6N} \xi_j \varphi_j \quad (3)$$

where  $\xi_j$  is the complex motion amplitude and the incident wave potential is

$$\varphi_0 = \frac{gA \cosh k(z+h)}{\omega \cosh kh} e^{-ikx \cos \beta - iky \sin \beta} \quad (4)$$

with  $A$  the wave amplitude,  $z$  the position in water (negative value in water),  $h$  the water depth,  $\beta$  the wave incident angle,  $g$  the gravity acceleration,  $\omega$  the frequency, and  $k$  the wave number. Diffraction potential,  $\varphi_D$  is due to the existence of the body (or bodies). Radiated potential,  $\varphi_j$  ( $j=1, \dots, 6N$ ,  $N$  is the number of rigid bodies) is due to the unit motions of the structures.

For solving the potentials, the boundary conditions shown in Table 1 must be satisfied. Substituting the Bernoulli equation, the pressure field under a progressive wave can be calculated by

$$\begin{aligned} p &= -i\omega\rho\varphi - \rho gz \\ &= -i\omega\rho [(\varphi_0 + \varphi_D) \\ &\quad + i\omega \sum_{j=1}^{6N} \xi_j \varphi_j] - \rho gz \end{aligned} \quad (5)$$

The forces and moments of the flow acting on the floating structure can be calculated by integrating the pressure over the wetted surface  $S_b$  as

$$\begin{aligned} \mathbf{F} &= -i\omega\rho \iint_{S_b} (\varphi_0 + \varphi_D) \mathbf{n} dS \\ &\quad + \omega^2 \rho \sum_{j=1}^{6N} \iint_{S_b} \xi_j \varphi_j \mathbf{n} dS \\ &\quad - \rho g \iint_{S_b} z \mathbf{n} dS \end{aligned} \quad (6)$$

$$\begin{aligned} \mathbf{M} &= -i\omega\rho \iint_{S_b} (\varphi_0 + \varphi_D) (\mathbf{r} \times \mathbf{n}) dS \\ &\quad + \omega^2 \rho \sum_{j=1}^{6N} \iint_{S_b} \xi_j \varphi_j (\mathbf{r} \times \mathbf{n}) dS \\ &\quad - \rho g \iint_{S_b} z (\mathbf{r} \times \mathbf{n}) dS \end{aligned}$$

Based on the solution of the forces/moments, the frequency-domain dynamic equation can be built as

$$\begin{aligned} F_i &= \sum_{j=1}^{6N} [-\omega^2 (M_{ij} + a_{ij}) + i\omega b_{ij} \\ &\quad + c_{ij}] \xi_j \\ &\quad (i = 1, \dots, 6N) \end{aligned} \quad (7)$$

where  $a_{ij}$ ,  $b_{ij}$  are the added mass and hydrodynamic damping coefficients,  $c_{ij}$  is the restoring force coefficient,  $F_i$  is the complex excitation amplitude, and  $\xi_i$  the complex motion amplitude.

Finally, the complex amplitude of the motions can be used to calculate RAOs (response amplitude operators),

Potential dynamic equation	Potentials to solve	Free surface condition at $z=0$	Body condition on $S_b$	Seabed condition at $z = -h$	Radiation condition ( $R \rightarrow \infty$ )
$\nabla^2 \varphi_D = 0$	$\varphi_D$	$g \frac{\partial \varphi_D}{\partial z} - \omega^2 \varphi_D$	$\frac{\partial \varphi_D}{\partial n} = -\frac{\partial \varphi_0}{\partial n}$	$\frac{\partial \varphi_D}{\partial z} = 0$	$\varphi_D = 0$
$\nabla^2 \varphi_j = 0$ ( $j = 1, \dots, 6N$ )	$\varphi_j$	$g \frac{\partial \varphi_j}{\partial z} - \omega^2 \varphi_j$	$\frac{\partial \varphi_j}{\partial n} = n_j$	$\frac{\partial \varphi_j}{\partial z} = 0$	$\varphi_j = 0$

Table 1: Boundary conditions for velocity potentials

$$H_i = \frac{\xi_i}{A} \quad (i = 1, \dots, 6N) \quad (8)$$

Further WEC frequency domain analysis information can be found in (Bosma et al. 2012). An outline of time domain WEC simulation can be found in (Bosma et al. 2013).

### 3.1. Numerical Modelling Software

For this study, ANSYS AQWA was used to perform the numerical analysis. AQWA-LINE was used for wave diffraction and radiation analysis, AQWA-LIBRIUM was used for equilibrium and stability analysis, and AQWA-NAUT was used for non-linear analysis in the time domain. Fig. 4 shows the geometry setup of the simulation.

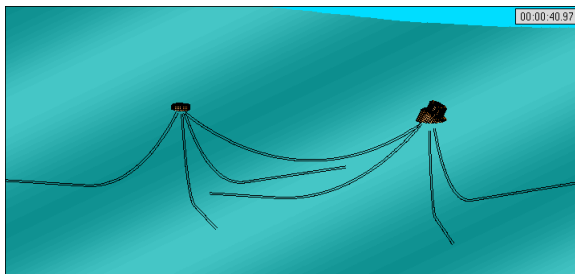


**Figure 4: Numerical model geometry, mooring, and umbilical setup**

Since the scaled models to be tested are 1:25 scale, the water depth was set to 25 m to match the 1 m scaled depth of basin testing water. The water density was set to 1000 kg/m<sup>3</sup> to match the fresh water density of the basin. For RAO analysis, each regular wave input was simulated for 4096 samples at a sampling rate of 32 Hz to match the physical wave basin testing parameters.

## 4. Wave Basin Testing

The first round of physical testing was conducted at the National Ocean Energy Test Facility at Beaufort Research, University College Cork Ireland. There were 17 days of wave basin time

with 11 different hardware configurations. Regular wave sets numbered 316, while irregular wave sets numbered 114. The tests were designed, in part, to investigate the influence of the mooring configuration and orientation of the bodies with relation to the incoming wave.

The testing facility has wave basin dimensions of 17.2 m width and 25 m length. The water depth is fixed at 1 m. The ocean wave generator is a flap type, with 40 individually controlled paddles allowing for a broad range of wave generating capabilities including regular and irregular single direction waves as well as directional spread waves (Edinburgh Designs 2014).

Regular wave tests were performed for 4096 samples and data was recorded at a sampling rate of 32 Hz. These were chosen to allow for a steady state condition to be reached for each output for every input wave. For tests in regular waves, three wave heights were chosen, 40 mm, 80 mm, and 120 mm which correspond to 1 m, 2 m, and 3 m respectively at full scale. The wave period was then swept from 0.8 s to 2.0 s in increments of 0.1 s corresponding to 4 s to 10 s full scale. The results from these tests were useful in obtaining RAO data for the bodies and load data from the mooring system.

Irregular wave tests were conducted for 11192 samples and data was recorded at 32 Hz. This was chosen based on the scaled down length of capture of ocean instrumentation buoys. Typically, instrumentation buoys take 20-30 minutes of wave data and calculate the sea state parameters as being the average over that time period. Allowing for ramp up times and Fourier analysis considerations the basin testing sample duration was chosen.

The final destination for the FPS is the Galway Bay test facility, near Spiddal, Ireland. Data from

the Sustainable Energy Authority of Ireland (SEAI) was used to emulate the conditions at this site (SEAI 2014) for the irregular wave tests. A scatter plot of percentage occurrence was referenced, and the best possible coverage of conditions was taken, to include the extremes.

#### 4.1. Experiments

In total, 11 experiments were undertaken. A new experiment was designated every time there was a change in the hardware configuration. Table 2 shows the bodies and orientations associated with each experiment. Fig. 5 shows the wave basin implementation for Exp9. The yellow in the background of the figure shows the wave paddles.

For Exp9, the bow line for both bodies is pointed toward the paddles which was chosen to be an orientation of  $60^\circ$  relative to the standard chosen orientation, for the purposes of the tests. For Exp6–Exp9 the distance between bodies was 3 m. For Exp8 and Exp9, the bodies made a line facing the paddles. For Exp6 and Exp7 there was an angle of  $45^\circ$  between the two bodies and the paddles.

Exp	Bodies	Orientation		Angle
		FPS	OWC	Between
Exp1	FPS	$0^\circ$		
Exp2	FPS	$60^\circ$		
Exp3	FPS	$30^\circ$		
Exp4	None			
Exp5	OWC		$60^\circ$	
Exp6	FPS&OWC	$0^\circ$	$60^\circ$	$45^\circ$
Exp7	FPS&OWC&Umb	$0^\circ$	$60^\circ$	$45^\circ$
Exp8	FPS&OWC	$60^\circ$	$60^\circ$	$0^\circ$
Exp9	FPS&OWC&Umb	$60^\circ$	$60^\circ$	$0^\circ$
Exp10	OWC		$60^\circ$	
Exp11	OWC		$60^\circ$	

**Table 2: List of Experiments with bodies and orientations listed**

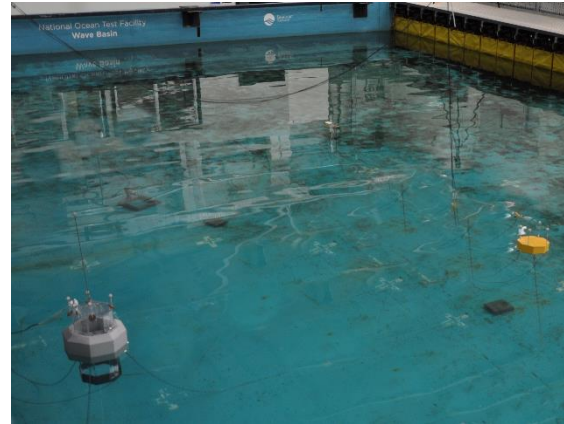


**Figure 5: Exp9 1:25 scaled testing in the Beaufort Research wave basin**

#### 4.2. Test and Measurement Equipment

Test and measurement data was captured using two physical systems which are synchronized. Data from sensors measuring water surface elevation, mooring force, and pressure in the OWC, were captured using a National Instruments CompactRIO data acquisition system (National Instruments 2014). Motion was captured by the Qualisys Motion Capture System (Qualisys 2014). All signals were sampled at a frequency of 32 Hz.

Wave measurement was achieved using two wire resistive type wave probes connected to an amplifier and the CompactRIO. A complete set of calibration wave data was created with the bodies removed from the basin which was used in the data analysis as input. Futek load cells were used to measure mooring line forces. The FPS had two 2 lbf load cells and one 10 lbf load cell attached at the body connection, one on each line. The OWC had one 10 lbf load cell attached at the bow mooring line. Pressure in the OWC chamber was measured using a Honeywell pressure sensor with a range of 0-14" H<sub>2</sub>O.

The Qualisys track manager software outputs two types of data files. One has three dimensional

(xyz) location information for each marker and each data step. The other provides six degrees of freedom measurements, namely x, y, z, roll, pitch, and yaw of a defined body (defined collection of markers). Data from the latter file was used in this analysis.

## 5. Key Findings

A key output from this work is the behaviour of the FPS and OWC under varying wave conditions. The RAO provides an insight into how a body will react for various period wave inputs. The results presented here are from Exp9, which included both bodies, namely the FPS and OWC, with the umbilical attached. A total of 16 regular waves were run with a wave height of approximately 80 mm (2 m full scale) and periods varying from 0.8 to 3.5 sec (4 to 17.5 sec full scale).

### 5.1. FPS RAOs

The key degrees of freedom of motion include the heave, surge, and pitch motion of the body. For the FPS, these motions should be minimized, if possible, to minimize the impact of on-board equipment and to provide a stable platform for WECs to connect to. Results of the RAO for the FPS is shown in Fig. 6 and are plotted versus the input waveform average measured period. Results from the wave basin testing were scaled using Froude scaling (introduced in (Newman 1977)) with a scaling factor of 25. AQWA simulations were done at full scale where the results are compared.

The heave motion of the FPS shows that it is essentially a wave follower for longer period waves, which AQWA predicts well. At shorter periods the wave basin testing shows attenuated heave motion of up to 15% where AQWA predicted closer to wave following.

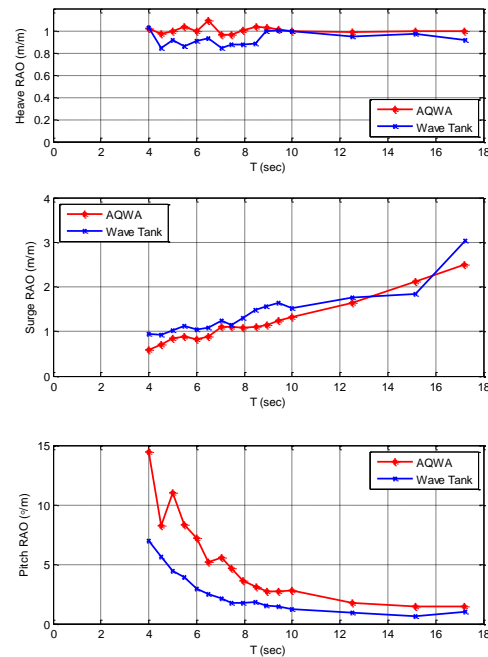


**Figure 6: FPS RAO results for heave, surge and pitch motions**

The surge motion of the FPS increases as the period increases as expected, both for wave basin results and AQWA results. The surge was up to 3 times the input wave height for the range of periods tested. AQWA under predicted this motion, by as much as 25%, but did show the same trend as the numerical model.

Pitch motion of the FPS decreased with longer periods as expected with a smaller slope. Numerical simulation over predicted pitch motion over all periods modelled, but again shows the same trend.

Analysis of the RAO data for interactions between the two bodies showed minimal impact on the motion of either device. Likewise with the umbilical, where its presence did not significantly impact the RAO heave, surge or pitch. These tests will be repeated at 1:10 scale to investigate further possible interactions.

### 5.2. OWC RAOs

For the OWC motion, the heave, pitch, and surge are also the critical motion to be analysed. For maximum power production, heave would be optimized to influence the change in water surface elevation within the chamber. Minimizing the surge and pitch motions are advantageous from a body stability standpoint. Fig. 7 shows the results of the RAO for the OWC.

Looking at the heave motion, for the wave basin testing, a slightly underdamped system response is found as expected. Apart from the lowest two periods tested, AQWA results show a similar response, with possibly a different peak period.

Surge motion generally increases with period as expected for both the basin testing and numerical simulation. AQWA under predicts the surge motion.

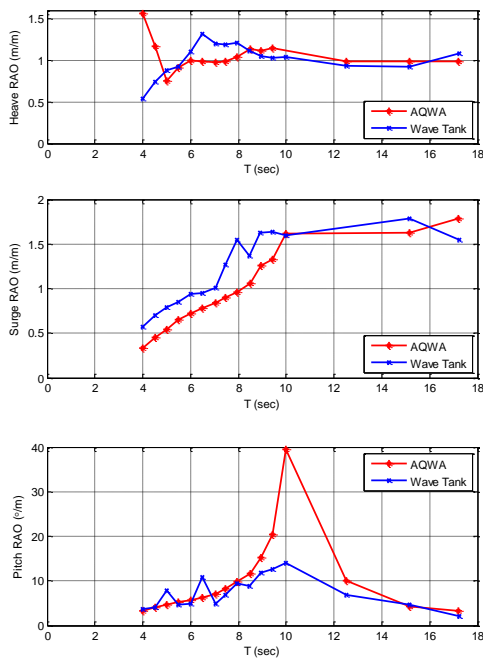


Figure 7: OWC RAO results for heave, surge and pitch motions

The pitch motion matches between AQWA and experimental testing for the lower and higher periods. Near the pitch resonance, however, AQWA greatly over predicts the response. This suggests a damping present in the physical system that the model is not accounting for.

### 5.3. Mooring Loads

Load cells were located on the mooring lines of each body at the connection point to the body. Fig. 8 shows the results from the same set of tests, namely Exp9. Results shown here are from the bow mooring line connection on each body. For the FPS, numerical modelling predictions of load match well, however, for longer period waves, the prediction diverges.

### 6. Conclusion

Wave basin testing at 1:25 scale of the Galway Bay Wave Energy Test Site was conducted at Beaufort Research, University College Cork, Ireland. Two bodies, namely the FPS and a generic OWC were tested by themselves and together including testing with an umbilical. RAO and mooring force results were shown for a case where both bodies were connected by an umbilical cable. These results were compared to numerical analysis.

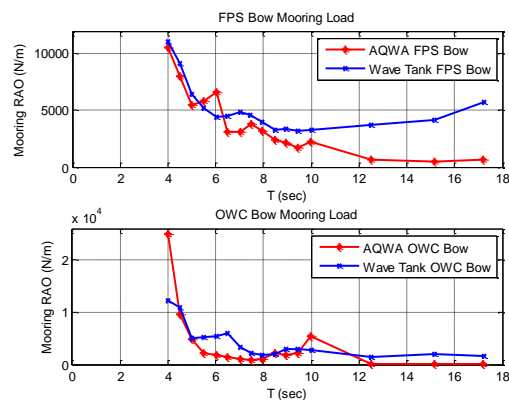


Figure 8: OWC RAO results for heave, surge and pitch motions

Based on these results, the numerical model will be refined. This research will continue with testing at the Plymouth University COAST wave lab at 1:10 scale. Comparison of results at different scales, additional mooring configurations including a compliant taut mooring, and improved numerical comparisons will be outputs of this continued research. Ultimately, this research will influence the final implementation of the Galway Bay Wave Energy Test Site.

### Acknowledgements

The author would like to thank University College Cork and Beaufort Research for supporting this research in part. The FPS and relevant infrastructure have been proposed, and funded by Science Foundation Ireland, Sustainable Energy Authority of Ireland, and the Irish Marine Institute. This research was also supported in part by the Department of Energy (DOE) Office of Energy Efficiency and Renewable Energy (EERE) Postdoctoral Research Awards under the EERE Water Power Program administered by the Oak Ridge Institute for Science and Education (ORISE) for the DOE. ORISE is managed by Oak Ridge Associated Universities (ORAU) under DOE contract number DE-AC05-06OR23100. All opinions expressed in this paper are the author's and do not necessarily reflect the policies and views of DOE, ORAU, or ORISE

### References

- Bosma. 2013. "On the Design, Modeling, and Testing of Ocean Wave Energy Converters," July. <http://ir.library.oregonstate.edu/xmlui/handle/1957/41003>.
- Bosma, Bret, T. Brekken, H. Tuba Ozkan-Haller, and Solomon C. Yim. 2013. "Wave Energy Converter Modeling in the Time Domain: A Design Guide." In *IEEE Conference on Technologies for Sustainability*. Portland, OR.
- Bosma, Bret, Zhe Zhang, Ted K.A. Brekken, H. Tuba Ozkan-Haller, Cameron McNatt, and Solomon C. Yim. 2012. "Wave Energy Converter Modeling in the Frequency Domain: A Design Guide." In *2012 IEEE Energy Conversion Congress and Exposition (ECCE)*, 2099–2106. doi:10.1109/ECCE.2012.6342553.
- Edinburgh Designs. 2014. "Flap Ocean Wave Generators | Edinburgh Designs." Accessed September 8. <http://www.edesign.co.uk/product/ocean-flap-wave-generator/>.
- Falnes, J. 2005. *Ocean Waves and Oscillating Systems: Linear Interactions Including Wave-Energy Extraction*. Cambridge: Cambridge University Press.
- Faltinsen, O. 1993. "Sea Loads on Ships and Offshore Structures." <http://www.cambridge.org/ie/academic/subjects/engineering/engineering-design-kinematics-and-robotics/sea-loads-ships-and-offshore-structures>.
- Holmes, B. 2012. "Tank Testing of Wave Energy Conversion Systems: EMEC: European Marine Energy Centre." Accessed December 3. <http://www.emec.org.uk/tank-testing-of-wave-energy-conversion-systems/>.
- Lettenmaier, T., E. Amon, and A von Jouanne. 2013. "Power Converter and Control System Developed in the Ocean Sentinel Instrumentation Buoy for Testing Wave Energy Converters." In *2013 IEEE Energy Conversion Congress and Exposition (ECCE)*, 344–51. doi:10.1109/ECCE.2013.6646721.
- Lewis, T. 2011. "The Status of Ocean Energy Development in Europe and Some Current Research Questions." In *OCEANS 2011*, 1–6.
- National Instruments. 2014. "National Instruments: Test, Measurement, and Embedded Systems." Accessed September 8. <http://www.ni.com/>.
- Newman, John. 1977. *Marine Hydrodynamics*. MIT Press.
- Qualisys. 2014. "Motion Capture – Mocap – Qualisys Motion Capture Systems." Accessed September 8. <http://www.qualisys.com/>.
- SEAI. 2014. "Galway Bay Wave and Weather Data." Accessed September 8. [http://www.seai.ie/Renewables/Ocean\\_Energy/Galway\\_Bay\\_Test\\_Site/Test\\_site\\_Wave\\_and\\_Weather\\_info.html](http://www.seai.ie/Renewables/Ocean_Energy/Galway_Bay_Test_Site/Test_site_Wave_and_Weather_info.html).